

Virtual admittance Based Current Control Strategy for Grid-connected inverters in Microgrid

Abstract. Integration the distributed energy resources into the microgrid is developed in a rapid pace. Conventionally, the voltage-source inverters in microgrid with sinusoidal current regulation are used in grid-connected mode. In this paper, a two-degree-of-freedom nonsinusoidal current control strategy is proposed for both the distributed power generation and power quality enhancement. The equivalent Thevenin-Norton circuit is presented to clarify the concept that the proposed strategy with virtual admittance leads to the power quality improvement. It is demonstrated that without any harmonic current sensor or additional compensating device, the harmonics of the voltages at the point of common coupling and currents in microgrid can be mitigated significantly. Time-domain performance evaluation results confirm the concept.

Streszczenie. Zazwyczaj przekształtnikowe źródła napięcia w mikrosieciach są połączane ze sterowaniem prądu sinusoidalnego. W artykule zaproponowano strategię kontroli prądu niesinusoidalnego z wykorzystaniem wirtualnej admittancji w celu poprawy jakości energii. (Strategia kontroli prądu w przekształtnikach dołączonych do mikrosieci bazująca na wirtualnej admittancji)

Keywords: Microgrid, grid-connected inverters, two-degree-of-freedom control, virtual admittance

Słowa kluczowe: mikrosiec, przekształtniki, wirtualna admittancja.

Introduction

The environmental concerns and electric utility deregulation promote the development of distributed generation (DG) in a rapid pace [1-5]. The high penetration of DG brings about a concept of the microgrid [4]. It is defined as a cluster of DG units (such as wind turbines and photovoltaics), storage devices and loads, which can operate in the grid-connected mode, autonomous mode, and ride-through between the two modes. Typically, the current-regulated voltage-source inverter used to provide the interface between the DG and the grid [6-7]. In most cases, the sinusoidal current regulation (SCR) with low distortion has been considered a defaulted control way for grid-connected inverters [8]. In fact, SCR stems from a common principle that grid-connected inverters should not inject harmonics into the grid, because these harmonics will cause the negative effects on the sensitive loads. On the other hand, there are so many nonlinear loads in the microgrid or utility networks that the harmonic pollution is still serious, even if the grid-connected inverters do not inject harmonics.

Conventionally, Harmonic mitigation can be achieved by active filter techniques. In general, these techniques employ the current harmonic extraction and control strategy on condition that harmonic sources are available at a certain location. In practice, however, it is not an effective solution because locating all harmonic sources is not an easy task in a real distributed system, and it's impractical to install active filters for every harmonic source.

IEEE Standard 1547 defines the ancillary services in distributed power generation systems. It is very interesting to integrate the power quality improvement function into the power generation units in microgrid. The objective of this paper is to develop a nonsinusoidal current regulation (NCR) of grid-connected inverters in microgrid, which not only inject the sinusoidal current for the power generation, but also absorb the harmonics from the microgrid for the power quality improvement with no need of positioning harmonic sources and installing additional compensating devices.

Strategy Description

Fig.1 illustrates the schematic diagram of the microgrid. It comprises of the primary energy sources (PV, wind, et al.) with optional energy storages, dc/dc or ac/dc converters and dc/ac inverters. The inverters can provide an interface for the flexible functions such as energy conversion and

power quality improvement. The inverter output may either feed the local loads independently in autonomous mode or in conjunction with the electric utility by static switch (STS) in grid connected mode. This paper will focus on the latter mode.

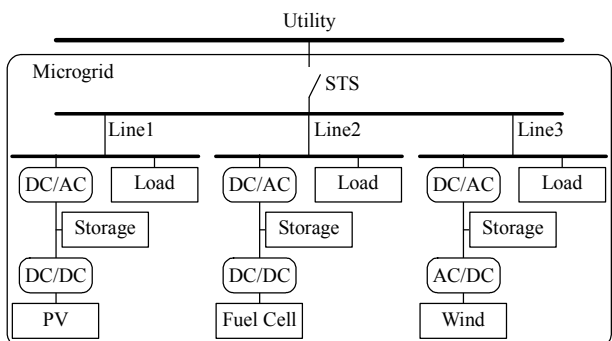


Fig.1. Schematic diagram of the microgrid

For simplicity, only the inverter is considered, and the rest of microgrid is modeled as another unit. As shown in Fig.2, the simplified model consists of the inverter, filter capacitor, local load and transmission line. Its equivalent Thevenin-Norton circuit is shown in Fig.2b, where I_1 represents the fundamental sinusoidal current regulation, while I_2 stands for the harmonic current regulation by the virtual admittance.

From Fig.2, the voltage at the point of common coupling (PCC) can be derived as follows:

$$(1) \quad U_{pcc} = \frac{1}{1 + Z_s Y + Z_s C_s} U_s + \frac{Z_s}{1 + Z_s Y + Z_s C_s} I_1$$

From (1), the harmonic components of the voltage at PCC can be obtained as:

$$(2) \quad U_{pcc_h} = \frac{1}{1 + Z_{sh} Y + Z_{sh} C_s} U_{sh}$$

Equation (2) indicates that the sinusoidal current regulation (SCR) with zero admittance ($Y = 0$) will lead to the harmonic-damping ratio of $1/(1 + Z_s C_s)$, while nonsinusoidal current regulation (NCR) with the virtual admittance Y will cause the increased harmonic-damping ratio of $1/(1 + Y Z_s + Z_s C_s)$. In other words, the larger admittance Y will lead to higher harmonic-damping ratio.

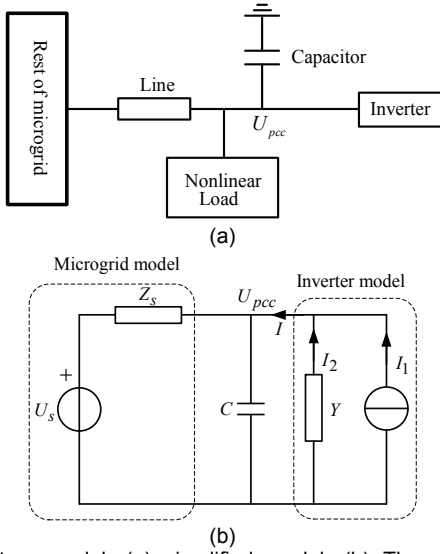


Fig.2 System model: (a) simplified model; (b) Thevenin-Norton equivalent circuit

In order to get the information of the nonsinusoidal current regulation, the linear control model of the grid-connected inverter is provided in Fig.3, where $A(s)$ is the admittance regulator, $C(s)$ is the current regulator, K is the PWM inverter gain, L and R is the interface inductor and its equivalent series resistor.

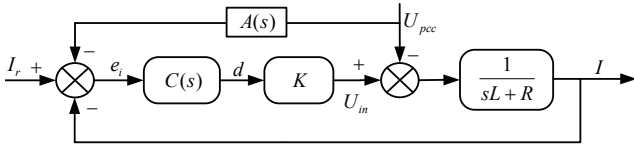


Fig.3 Linear control model of grid-connected inverter

Nonsinusoidal current regulation of the grid-connected inverter can be derived from Fig.3 as follows:

$$(3) \quad I(s) = \frac{KC(s)}{Ls + R + KC(s)} I_r(s) - \frac{1 + KC(s)A(s)}{Ls + R + KC(s)} U_{pcc}(s)$$

$$\text{where } I_1(s) = \frac{KC(s)}{Ls + R + KC(s)} I_r(s)$$

$$I_2(s) = -\frac{1 + KC(s)A(s)}{Ls + R + KC(s)} U_{pcc}(s)$$

Equation (3) indicates that the sinusoidal current regulation $I_1(s)$ and harmonic current regulation $I_2(s)$ with the virtual admittance can be adjusted independently via the regulator $C(s)$ and $A(s)$, which implies that two-degree-of-freedom control is achieved.

The virtual admittance can be derived from (3) as:

$$(4) \quad Y(s) = \frac{1 + KC(s)A(s)}{Ls + R + KC(s)}$$

In this paper, an admittance regulator is proposed as follows:

$$(5) \quad A(s) = \frac{a(s^2 + \omega_0^2)}{s^2 + \omega_c s + \omega_0^2}$$

Fig. 4 shows the virtual admittance in case of different values of "a". It can be observed that the larger "a" leads to higher virtual admittance, and thus higher harmonic-damping ratio.

In order to further clarify the effectiveness of the proposed method, the harmonic damping factor is defined as $k_d = 1/(1 + Z_{sh}Y + Z_{sh}Cs)$ from (2). The frequency domain analysis of the factor k_d is illustrated in Fig.5, from which it is

clear that the larger "a" leads to the higher harmonic-damping ratio.

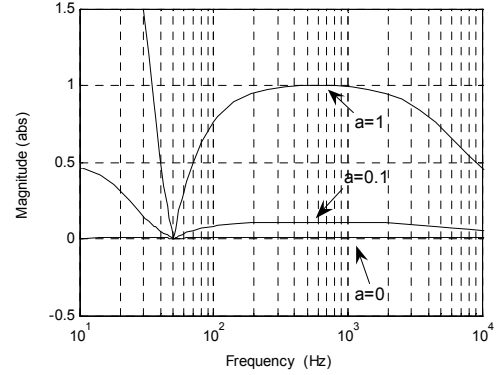


Fig.4 Virtual admittance in case of different values of "a"

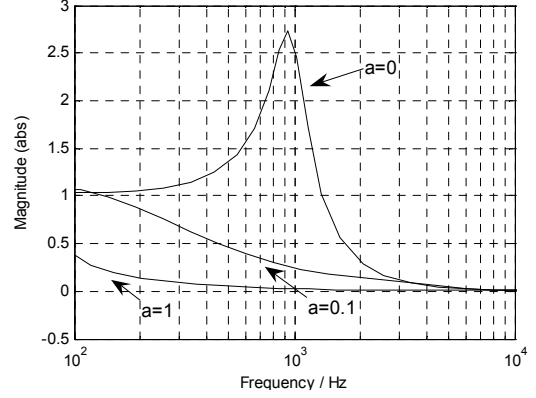


Fig.5 Frequency domain analysis for k_d

Performance Evaluation

The performance evaluation of the proposed scheme has been carried out based on time-domain simulation in MATLAB/Simulink environment. The system parameters are given in appendix.

Case I. Single-phase applications

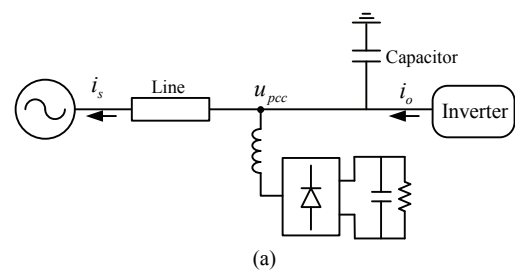
Fig.6 shows the simulation schematic diagram and the test results. Table I offers a quantitative analysis of the total harmonic distortion for the results.

Fig.6 and Table I indicate that higher harmonic-damping ratios of both PCC voltage harmonics and microgrid current harmonics are achieved with the larger "a". That is to say, higher virtual admittance leads to the lower harmonic distortion of PCC voltages and microgrid currents.

Case II. Three-phase applications

Fig.7 illustrates the simulation schematic diagram and the test results. Table II offers a quantitative analysis of the total harmonic distortion for the test results.

As shown in Fig.7 and Table II, the proposed nonsinusoidal current regulation with virtual admittance can achieve the desired harmonic damping in the three-phase microgrid as well.



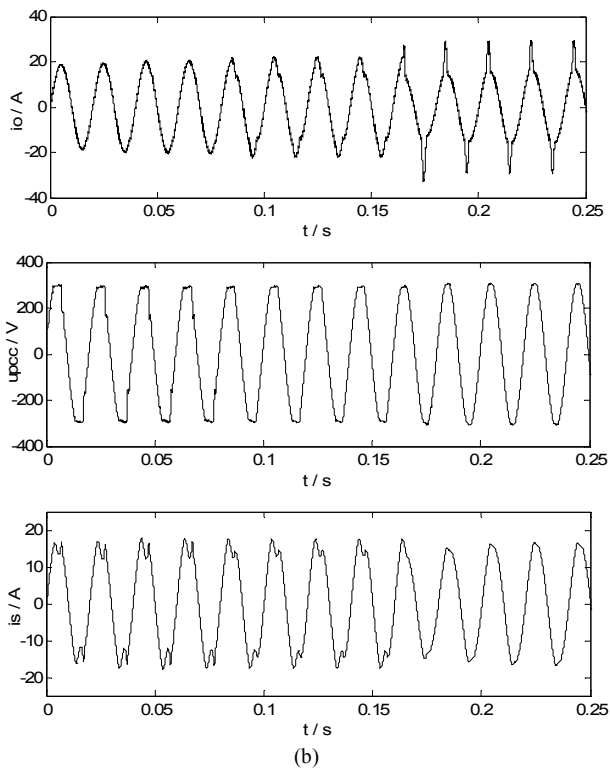
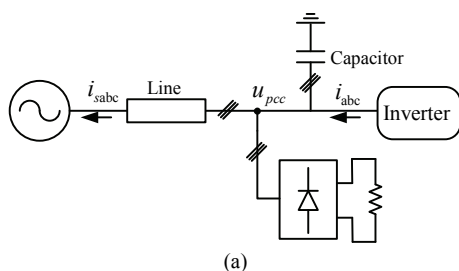


Fig.6 Time-domain simulation: (a) simulation schematic diagram; (b) test results.

Table I. Harmonic analysis for voltages and currents

	THD	i_o	U_{pcc}	i_s
$a = 0.0$ 0~85ms		1.63%	8.21%	16.88%
$a = 0.1$ 85~165ms		9.28%	5.64%	15.07%
$a = 1.0$ 165ms~250ms		23.50%	1.55%	3.87%



(a)

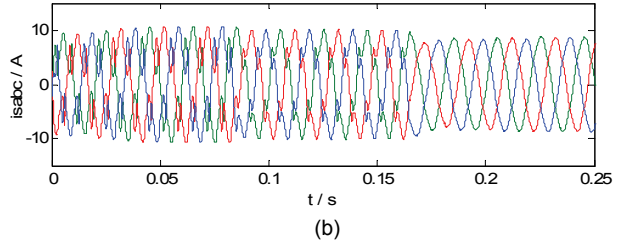
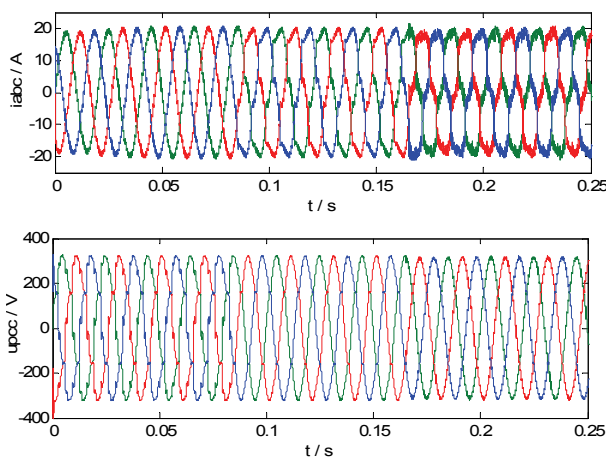


Fig.7 Time-domain simulation: (a) simulation schematic diagram; (b) test results

Table II. Harmonic analysis for voltages and currents

	THD	i_{abc}	U_{pcc}	i_{sabc}
$a = 0.0$ 0~85ms	2.77%	12.91%	33.16%	
	2.79%	12.83%	33.12%	
	2.79%	12.88%	33.13%	
$a = 0.1$ 85~165ms	11.72%	6.87%	22.52%	
	11.79%	6.85%	22.46%	
	11.76%	6.86%	22.48%	
$a = 1.0$ 165ms~250ms	18.05%	1.76%	3.97%	
	18.15%	1.71%	3.90%	
	18.08%	1.73%	3.93%	

Conclusion

This paper has attempted to make two major contributions: 1) Development of a nonsinusoidal current regulation for grid-connected inverters in microgrid based on virtual admittance concept. 2) Offering two degrees of freedom control structure for the nonsinusoidal current regulation. From the paper's theoretical analysis and evaluation results, several important conclusions can be reached.

- The proposed nonsinusoidal current regulation can achieve the superior harmonic damping of both PCC voltages and microgrid currents over the conventional sinusoidal current regulation with no impact on the fundamental power generation due to two degrees of freedom control structure.

- Higher virtual admittance leads to lower harmonic distortion and higher harmonic-damping ratio. In practice, however, the virtual admittance should be limited by the inverter current ratings.

- The unique feature of the proposed method is that, it only depends on the local voltage measurement, and does not require any harmonic source/load current sensor or any other external compensating device such as active filters. It is very promising for the real distributed system, especially the microgrid applications, where positioning every harmonic source is impractical.

- The proposed method can be applied to both single-phase and three-phase microgrids.

REFERENCES

- [1] B.V. Mathiesen, H. Lund. Comparative analyses of seven technologies to facilitate the integration of fluctuating renewable energy sources. *IET Renewable Power Generation*, vol.3, no.2, pp. 190-204, 2009.
- [2] A. Hajizadeh, M. A. Golkar. Fuzzy neural control of a hybrid fuel cell/battery distributed power generation system. *IET Renewable Power Generation*, vol.3, no.4, pp.402-414, 2009.
- [3] A. K. Saha, S. Chowdhury, S. P. Chowdhury, Y. H. Song. Application of solid-oxide fuel cell in distributed power generation. *IET Renewable Power Generation*, vol.1, no.4, pp.193-202, 2007.
- [4] Y. W. Li, D. M. Vilathgamuwa, and P. C. Loh. Design, analysis, and real-time testing of a controller for multibus microgrid system. *IEEE Transactions on Power Electronics*, vol. 19, no. 5, pp. 1195-1204, Sep. 2004.

- [5] D. Mahinda Vilathgamuwa, Poh Chiang Loh, Yunwei Li. Protection of microgrids during utility voltage sags. *IEEE Transactions on Industrial Electronics*, vol. 53, no. 5, pp. 1427–1436, 2006.
- [6] Sudipta Chakraborty, Manoja D. Weiss, M. Godoy Simões. Distributed intelligent energy management system for a single-phase high-frequency AC microgrid. *IEEE Transactions on Industrial Electronics*, vol. 54, no.1, pp. 97-109, 2007.
- [7] Josep M.Guerrero, Lijun Hang, Javier Uceda. Control of distributed uninterruptible power supply systems. *IEEE Transactions on Industrial Electronics*, vol. 55, no. 8, pp. 2845-2859, 2008.
- [8] R. Majumder, A. Ghosh, G. Ledwich, F. Zare. Load sharing and power quality enhanced operation of a distributed microgrid. *IET Renewable Power Generation*, vol.3, no.2, pp. 109-119, 2009.
- [9] A. G. Madureira, J. A. Peças Lopes. Coordinated voltage support in distribution networks with distributed generation and microgrids. *IET Renewable Power Generation*, vol.3, no.4, pp.439-454, 2009.
- [10] J. A. M. Bleijs. Wind turbine dynamic response-difference between connection to large utility network and isolated diesel micro-grid. *IET Renewable Power Generation*, vol.1, no.2, pp. 95-106, 2007.
- [11] Qingrong Zeng, Liuchen Chang. An advanced SVPWM-based predictive current controller for three-phase inverters in distributed generation systems. *IEEE Transactions on Industrial Electronics*, vol.55, no.3, pp. 1235-1246, 2008.
- [12] Tusitha Abeysekera, C. Mark Johnson, David J. Atkinson, Matthew Armstrong. Suppression of line voltage related distortion in current controlled grid connected inverters. *IEEE Transactions on Power Electronics*, vol. 20, no. 6, pp. 1393–1401, 2005.
- [13] M. Liserre, R. Teodorescu, and F. Blaabjerg. Multiple harmonics control for three-phase grid converter systems with

the use of PI-RES current controller in a rotating frame. *IEEE Transactions on Power Electronics*, vol. 21, no. 3, pp. 836–841, 2006.

Appendix

The system parameters are given as follows:

Table III. Single-phase system parameters

System elements	Value
DC bus	400V
Microgrid voltage	220V/50Hz
Line impedance	6mH
Filter capacitor	4.7uF
Interface inductor	3mH
Switching frequency	25kHz
Nonlinear load (resistor)	200 Ω
Nonlinear load (capacitor)	1000uF

Table IV. Three-phase system parameters

System elements	Value
DC bus	800V
Microgrid voltage	380V/50Hz
Line impedance	6mH
Filter capacitor	4.7uF
Interface inductor	3mH
Switching frequency	25kHz
Nonlinear load (resistor)	50 Ω

Authors,

Cao Hai-yan, Department of Information Engineering, Shijiazhuang University of Economics, Shijiazhuang 050031, China. Email: beatles888@126.com